Diabetologia (2000) 43: 609–624

Diabetologia

Modelling of the MHC II allele I-A^{g7} of NOD mouse: pH-dependent changes in specificity at pockets 9 and 6 explain several of the unique properties of this molecule

A. K. Moustakas[1], **J. Routsias**[2, 3], **G. K. Papadopoulos**[1]

[1] Laboratory of Biochemistry and Biophysics, Faculty of Agricultural Technology, Technological Educational Institute of Epirus, Arta, Greece
[2] Laboratory of Immunology, Department of Internal Medicine, University of Ioannina Medical School, Ioannina, Greece
[3] Current address: Laboratory of Pathophysiology, Medical School University of Athens, Athens, Greece

Abstract

Aims/hypothesis. We modelled the three-dimensional structure of I-A^{g7}, the chief genetic component of diabetes in non-obese diabetic mice, to understand the unusual properties of this molecule.
Methods. Modelling was done, in complex with established antigenic peptides, based on the structure of I-A^{k}.
Results. The selectivity of the I-A^{g7} molecule changes greatly at pockets 9 and 6 but hardly at all at pockets 1, 4 and 7, between endosomal pH (5.0) and extracellular pH (7.0), in agreement with previous results. This selectivity is attributed to the unique combination of β9His, β56His and β57Ser. The positive charges in and around pocket 9 at pH 5, favour binding by negatively charged residues. At pH 7 however, the uncharged α68, β9 and β56 histidines favour the accommodation of the bulky residues lysine, arginine, phenylalanine and tyrosine at pocket 9. The combination of β9His and α66Glu is responsible for the pH-dependent selectivity at pocket 6. Furthermore, the lack of repulsion between β56His and α76Arg at pH 7 leads to a more stable ternary complex.
Conclusion/interpretation. These results reconcile previous conflicts over the peptide binding ability of I-A^{g7} and its motif. They furthermore provide possible explanations for the short lifetime of cell-surface I-A^{g7} complexes in vivo, the higher threshold of thymic negative selection and inherent self-reactivity shown by immunocytes in these mice and the protection from diabetes afforded to them by several transgenically expressed mouse class II alleles. This contributes to an understanding of the pathogenesis of Type I (insulin-dependent) diabetes mellitus in this animal. [Diabetologia (2000) 43: 609–624]

Keywords Autoimmunity, I-A^{g7} molecule, MHC class II structure, protein modelling, NOD mice, Type I diabetes mellitus.

The non-obese diabetic (NOD) mouse is an animal model of Type I (insulin-dependent) diabetes mellitus [1, 2]. Extensive work on this model has shown that the chief genetic determinant of diabetes is the unique MHC class II allele of this mouse, termed I-A^{g7} [2, 3]. The MHC class II molecules exist on professional antigen-presenting cells (APCs, i. e. dendritic cells, B lymphocytes and macrophages). They capture processed antigen fragments, forming complexes that are presented to CD4^{+} helper T-cells. Because of a deletion in their *H-2/I-Eα* gene, NOD mice do not express an I-E molecule [4]. Sequencing of the I-A^{g7} molecule showed a number of remarkable features in its beta chain; a histidine in position 56 and a serine in position 57 [5]. The histidine is unique to I-A^{g7} of all known mouse, rat, porcine, bovine and human MHC class II alleles [6, 7]. The β57Ser is unique to the I-A^{g7} of all mouse MHC class II alleles but is

Received: 9 August 1999 and in revised form: 27 January 2000

Corresponding author: G. K. Papadopoulos, PhD, Laboratory of Biochemistry and Biophysics, Faculty of Agricultural Technology, Technological Educational Institute of Epirus, GR-47100 Arta, Greece

Abbreviations: aa, Amino acid; APC, antigen-presenting cell; CLIP, class II associated invariant chain peptide; GAD, glutamic acid decarboxylase; HEL, hen egg white lysozyme; hsp60, heat-shock protein 60; IC_{50}, concentration yielding 50% inhibition in competitive binding experiments using soluble I-A^{g7}; NOD, non-obese diabetic; p, pocket, position.

also found in a number of such alleles in rat and humans [6]. Specifically in humans, the β57 position is polymorphic and has been identified early on as one of the key determinants of diabetes susceptibility, which is associated with the absence of aspartate in susceptible HLA-DQ alleles [8]. The alpha chain of I-A^{g7} is identical to that of I-A^{d} [1, 4].

Establishing the three-dimensional structure of seven different MHC class II alleles, DR1, DR2, DR3, DR4, I-E^{k}, I-A^{d} and I-A^{k}, each in complex with an antigenic peptide, has allowed the delineation of the binding rules and motifs of antigenic peptides to such molecules [9–15]. The overall shape of mouse and human MHC class II alleles is very similar. In the antigen-binding domain, α1β1, the binding groove is formed by two antiparallel α-helical "walls" to either side of a β-pleated sheet floor. The antigenic peptide fits into the groove with its backbone nearly parallel to the axes of the α-helical walls and its amino and carboxy termini projecting out of the two openings of the groove. The specificity in the binding of various residues of the antigenic peptide is provided by several depressions in the antigen-binding groove, termed "pockets". The binding and crystallographic data show unequivocally that in human HLA-DR molecules, and their mouse counterparts H-2/I-E, the pockets for the binding of residues from the antigenic peptide occur at relative positions 1, 4, 6, 7 and 9, designated as pocket (p)1, p4 etc. [16]. Bound peptides isolated from MHC II molecules can be 11–22 residues long, containing the nonamer core flanked by a few to several amino acids on either side [16]. The non-specific mode of peptide binding is facilitated by the several strategically positioned polar residues. Many of them are invariant and mostly they are from the α1 and β1 helices that form hydrogen bonds to select amide and carbonyl groups of the bound antigenic peptide. The only structural features unique to mouse I-A alleles occur in the α1β1 antigen binding domain; a β-bulge at position α9 and an amino acid insertion at β84 a (for an explanation of notation see Materials and methods and Fig. 1), 10 residues earlier than assumed previously [6, 14, 15, 17].

Contrasting findings by several laboratories range from the unique I-A^{g7} molecule being a poor [18] or a good binder [19–27] of antigenic peptides with sharply varying specificities at pockets 6 and 9 [21–23]. One study found purified I-A^{g7} to be a very weak binder of several antigenic peptides at pH 5.5 [18] but three other studies done at pH 4.5 to 5.5 and using mostly different peptides, reported binding affinities in the low to mid-μmol/l range [24–26]. Another study tested binding at pH 5 of peptide 12 from mouse heat-shock protein 60 (hsp60) to activated, and then paraformaldehyde-fixed, peritoneal macrophages of NOD mice, thus deriving a motif for the various pockets of the I-A^{g7} allele [21]. In a subsequent binding/stability study, also at pH 5, the same group reported similar results [23]. By contrast, binding of the immunogenic [28] hen egg white lysozyme (HEL) 10–22 peptide and several of its variants to purified I-A^{g7} molecules was tested in another study at pH 7, where a higher affinity [concentration for 50 % inhibition of binding (IC_{50}) = 295 nmol/l] for the peptide and a different motif were established [22]. These peptides were also tested for activation of a HEL10–22-specific, I-A^{g7}-restricted T-cell hybridoma [22]. The stability of I-A^{g7} molecules in vivo [18, 21, 23, 29–31] and in vitro [21–23, 26] has also been variably reported by different groups, either as very low in vivo [18, 29–31] and in vitro [18, 26], or high in vivo [21, 23]. We have taken into account the results of these binding studies at different pH values and carried out homology modelling of I-A^{g7} complexed to this antigenic peptide from HEL, as well as to established epitopes of the primary autoantigen glutamic acid decarboxylase (GAD) [24, 25, 32–42], the GAD homologous peptide from the C2 protein of Coxsackie B4 viral strain [43], the autoantigens insulin beta chain [44, 45] and hsp60 peptide 12 [21, 23], antigenic peptides from sperm whale, equine, and mouse myoglobins [46, 47], class II invariant chain peptide (CLIP) and I-A^{g7}-derived and I-Eα-derived immunogens [25–27], carboxypeptidase H [18, 26] and two I-A^{g7}-eluted peptides derived from mouse serum albumin and transferrin [19, 26].

Materials and methods

Coordinates of crystal structure, I-A^{g7} and peptide alignments and amino acid conformations for modelling. The coordinates of the I-A^{k} complexed to the HEL50–62 peptide [14] were obtained from Dr. D. Fremont and the Protein Data Bank (access code 1iak). They include the positions of residues 1–181 of the alpha chain and 5–190 of the beta chain as well as the coordinates of the bound HEL50–62 peptide and those of the linker peptide connecting the carboxy-terminus of the HEL peptide to the amino terminus of the beta chain. The alignment of I-A^{g7} and I-A^{k} molecules was done as in [14]. (See also Fig. 1 of this work). The numbering scheme used for the alpha and beta chains of I-A^{g7} was identical to the one adopted by these authors. Modelling work was done on an Indy computer workstation (Silicon Graphics, Mountain View, Calif., USA) using the programs Insight II/Discover, versions 95.0/2.9.7/3.0 (Biosym Technologies/Molecular Simulations, San Diego, Calif., USA). The I-A^{g7} alpha chain is 87 % identical to the I-A^{k} alpha chain in the α1 domain, and 97 % identical in the α2 domain. The I-A^{g7} β chain is 88 % identical to the I-A^{k} beta chain in the β1 domain and 96 % identical in the β2 domain, a much higher homology than shown to DR1 [48]. There were no amino acid substitutions in the sequence that would be expected to greatly change the local secondary structure of I-A^{g7}. The individual amino acid conformations were automatically chosen by the modelling program from a library of rotamers contained in it, using the most suitable rotamer for each case. The antigenic peptides used to occupy the respective positions in the groove were those reported as immunogenic in NOD mice, either in spontaneous or induced responses [21–28, 32–47].

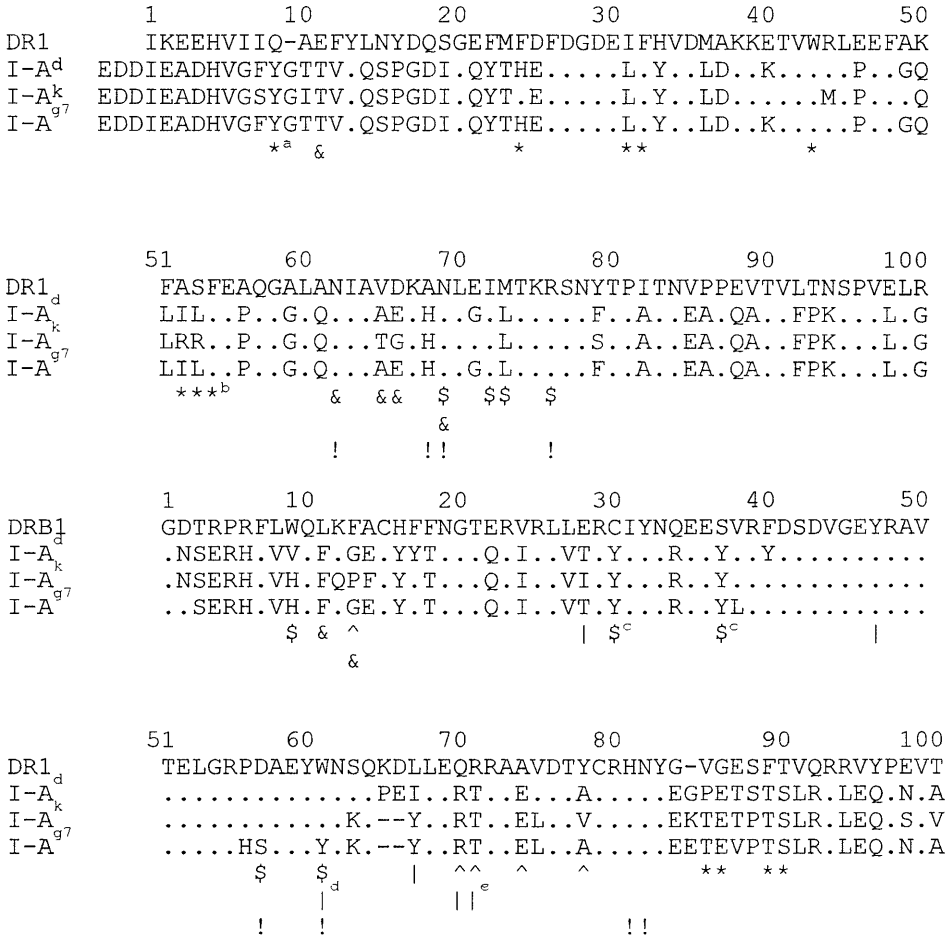

Fig. 1 A, B. Amino acid sequences of the alpha (**A**) and beta (**B**) chains of the mouse I-A^{d}, I-A^{k} an I-A^{g7} alleles and DR1 in the α1β1 domain. The numbering used in the alpha chain and the beta chain is that proposed previously [14]. Code: .: Identity; –: no amino acid in corresponding position (specifically, α9a and β84a); !: intermolecular hydrogen bonds between MHC class II molecule and the bound antigenic peptide; *: residues forming p1; ^: residues forming p4; &: residues forming p6; |: residues forming p7; $: residues forming p9. [a]In DR, α7Ile is part of p1 whereas in I-A alleles the equivalent residue is α9Tyr. [b]α52 and α54 are part of p1 only in I-A alleles. In I-A^{k} alone α53 is also part of p1. [c]In I-A^{g7}, modelling shows the β30 and β37 Tyr residues to participate in p9 when this pocket is occupied by Arg/Lys/Phe/Tyr at pH 7. [d]In I-A^{g7}, modelling shows that β61Tyr participates in the formation of both p7 and p9. [e]In I-A^{g7}, modelling shows that β70Arg and β71Thr participate in the formation of p7, while in DR1, β71Arg is part of both pockets 4 and 7 and β70Gln is part of pocket 4 only. In the crystal structure of I-A^{k} both residues are part of p7 while in the crystal structure of I-A^{d}, β71Thr is part of p7 and β70Arg does not seem to participate in the formation of either pocket

The ionisation state of amino acid side-chains was that at pH 5, the approximate pH of the endosomal compartment or pH 7. The register for fitting each peptide into the groove was resolved by using the results of the extensive peptide competition binding studies to I-A^{g7} at pH 5 and pH 7 [21, 22]. The respective motifs are called by us, but not by the authors of these works, "pH 5 motif" and "pH 7 motif". The respective registers for fitting the antigenic peptides at each pH into the groove were decided by us on the basis of the motif studies (Table 1). Energy minimisation of the I-A^{g7}-peptide complexes was done for most peptides in at least two different registers and at two different pH values (5 and 7). As the I-A^{k}-HEL50–62 coordinates included a 13-mer peptide, all peptides used in the energy minimisation studies (except known cases of tested shorter peptides) included a nonamer core (p1-p9) and, wherever possible, two residues on either side of the core amino termini and carboxy termini.

The ionisation state of the three histidines (α68, β9 and β56) in and around p9 at the two pH values, was decided as follows: at pH 5, α68His and β56His are completely exposed to solvent and β9His, although at the bottom of p9, can still come in contact with the solvent, when an acidic residue is at p9 (see Results). The crystal structures of I-A^{k}/I-A^{d} show that there is ample room between the p9Ser/Ala residue and β9His/Val respectively for at least two solvent molecules to interpose [14, 15]. Thus β9His of I-A^{g7} could be in contact with bulk solvent. Therefore, β9His will be 90 % uncharged at pH 7 (pK_a = 6.0).

Energy minimisation. Energy minimisation was accomplished by the steepest gradient method first, followed by the conjugate gradient method provided by the program Discover. The minimisation procedure went through 1000 cycles for each method. In the first 50 to 100 cycles of each minimisation the energy of the molecule dropped considerably but by the end of each run there were only very small changes in the energy values. Extending the number of steps in the conjugate gradient stage to 10 000 for a number of I-A^{g7}-peptide complexes

Table 1. Minimised energy values for I-A^{g7}-antigenic peptide complexes at pH 5 and pH 7 in registers fulfilling each motif

Name of antigen and/or peptide designation/peptide sequence	Amino acid sequence and register of binding 1 4 6 7 9	Motif pH	Minimised Energy at pH 5 kcal/mol	Minimised Energy at pH 7 kcal/mol	References where given peptide is shown to be antigenic for the NOD mouse[a]
HEL					[22[b], 28]
8–20	L A **A** A M **K** R **H** **G** L **D** N Y	5.0	1510	1493	
10–22	A A **M** **K** R **H** **G** **L** **D** N **Y** R G	7.0	1510	1414	
10–22p9F	A A **M** **K** R **H** **G** **L** **D** N **F** R G	"		1426	
10–22p9K	A A **M** **K** R **H** **G** **L** **D** N **K** R G	"		1416	
10–22p9R	A A **M** **K** R **H** **G** **L** **D** N **R** R G	"		1377	
10–22p9W	A A **M** **K** R **H** **G** **L** **D** N **W** R G	"		1465	
10–22p9A	A A **M** **K** R **H** **G** **L** **D** N **A** R G	"		1442	
10–22p9L	A A **M** **K** R **H** **G** **L** **D** N **L** R G	"		1441	
10–22p6M	A A **M** **K** R **H** G **MD** N **Y** R G	7.0		1406	
10–22p6I	A A **M** **K** R **H** G **I** **D** N **Y** R G	"		1416	
10–22p6V	A A **M** **K** R **H** G **V** **D** N **Y** R G	"		1417	
10–21	A A **M** **K** R **H** **G** **L** **D** N **Y** R	7.0		1455	
10–20	A A **M** **K** R **H** **G** **L** **D** N **Y**	"		1464	
10–19	A A **M** **K** R **H** **G** **L** **D** N	"		1459	
10–18	A A **M** **K** R **H** **G** **L** **D**	"		1488	
10–17	A A **M** **K** R **H** **G** **L**	"		1507	
10–16	A A **M** **K** R **H** G	"		1511	
10–15	A A **M** **K** R **H**	"		1520	
11–22	A **M** **K** R **H** **G** **L** **D** N **Y** R G	"		1436	
12–22	**M** **K** R **H** **G** **L** **D** N **Y** R G	"		1441	
13–22	K R **H** **G** **L** **D** N **Y** R G	"		1456	
14–22	R **H** **G** **L** **D** N **Y** R G	"		1508	
15–22	**H** **G** **L** **D** N **Y** R G	"		1482	
16–22	G **L** **D** N **Y** R G	"		1489	
17–22	**L** **D** N **Y** R G	"		1493	
Murine hsp60 Peptide 12					[21, 23]
169–181	A Q **V** A T **I** S **A** **N** G **D** K D	5.0	1501	1480	
169–181p9A	A Q **V** A T **I** S **A** **N** G **A** K D	"	1515		
169–181p9M	A Q **V** A T **I** S **A** **N** G **M** K D	"	1510		
169–181p6E	A Q **V** A T **I** S **E** **N** G **D** K D	"	1411		
169–181p6T	A Q **V** A T **I** S **T** **N** G **D** K D	"	1448		
169–181p7R	A Q **V** A T **I** S **A** **R** G **D** K D	"	1440		
169–180	A Q **V** A T **I** S **A** **N** G **D** K	5.0	1504		
170–180	Q **V** A T **I** S **A** **N** G **D** K	"	1521		
169–180p-2K	K Q **V** A T **I** S **A** **N** G **D** K	"	1546		
169–180p1A	A Q **A** A T **I** S **A** **N** G **D** K	"	1490		
169–180p1E	A Q **E** A T **I** S **A** **N** G **D** K	"	1471		
169–180p10A	A Q **V** A T **I** S **A** **N** G **D** A	"	1474		
169–180p9Y	A Q **V** A T **I** S **A** **N** G **Y** K	"	1521		
Peptide 437–460					
449–460	P A **L** D S **L** K **P** **A** N **E** D	5.0	1447	1504	
Human hsp60 Peptide 449–460					[21, 23]
449–460	P A **L** D S **L** T **P** **A** N **E** D	5.0	1461	1483	
Murine GAD65 Peptide 14 (aa202–221)					[40]
207–219	Y E **I** A P **V** F **V** **L** L **E** Y V	5.0	1564	1609	
208–220	E I **A** P V **F** V **L** **L** E **Y** V T	7.0	1612	1631	
Peptide 15 (aa217–236 or 221–235)[c]					[24, 38, 40]
216–228	L E **Y** V T **L** K **K** **M** R **E** I I	5.0	1545	1545	
217–227	**E** Y V **T** L **K** **K** M **R** E I	7.0	1585	1532	
221–232	L **K** K M **R** E **I** **I** G **W** P G	"	1627	1622	
Peptide 17 (aa247–266)					[33, 42, 43]
254–266	A R **Y** K M **F** P **E** **V** K **E** K G	5.0	1538	1526	
255–267	R Y **K** M F **P** E **V** **K** E **K** G M	7.0	1672	1643	
253–265	I A **R** Y K **M** F **P** **E** V **K** E K	"	1661	1674	
Peptides 286–300 (aa286–300) and 290–309 (p290)					[24, 42]
287–299	K G **A** A A **L** G **I** **G** T **D** S V	5.0	1515	1549	
295–307	G T **D** S V **I** L **I** **K** C **D** E R	"	1503	1498	
296–308	T D **S** V I **L** I **K** **C** D **E** R G	"	1401	1432	
293–305	G I **G** T D **S** V **I** **L** I **K** C D	7.0	1557	1520	
297–309	D S **V** I L **I** K **C** **D** E **R** G K	"	1745	1715	
Peptide 401–415					[24]
401–413	P L **Q** C S **A** L **L** **V** R **E** E G	5.0	1438	1454	
402–414	L Q **C** S A **L** L **V** **R** E **E** G L	"	1423	1474	
401–412	P **L** Q S **S** A **L** **L** V **R** E E	7.0	1660	1658	

Table 1. Continued

Name of antigen and/or peptide designation/peptide sequence	Amino acid sequence and register of binding 1 4 6 7 9	Motif pH	Minimised Energy at kcal/mol		References where given peptide is shown to be antigenic for the NOD mouse[a]
			pH 5	pH 7	
Peptide 34 (aa509–528)					[33, 35, 36, 39, 41]
507–519	WF **V** P P **S** L **R T** L **E** D N	5.0	1573	1568	
508–520	F V **P** P S **L** R **T L** E **D** N E	"	1470	1521	
510–522	P P **S** L R **T** L **E D** N **E** E R	"	1358	1418	
511–523	P S **L** R T **L** E **D** N **E** E R M	"	1382	1429	
512–524	S L **R** T L **E** D **N E** E **R** M S	7.0	1592	1610	
Peptide 35 (aa524–543)					[33, 37, 39, 41]
529–541	V A **P** V I **K** A **R M M E** Y G	5.0	1581	1564	
528–540	K V **A** P V **I** K **A R** M **M** E Y	"	1647	1671	
524–536	S R **L** S K **V A P V** I **K** A R	7.0	1654	1599	
526–538	L S **K** V A **P** V **I K** A **R** M M	"	1861	1814	
530–542	A P **V** I K **A** R **M M** E **Y** G T	"	1556	1542	
Peptide 36 (aa539–558)					[33]
542–554	T T **M** V S **Y** Q **P L** G **D** K V	5.0	1593	1601	
545–557	V S **Y** Q P **L** G **D K** V **N** F F	"	1620	1646	
537–549	M M **E** Y G **T** T **M V** S **Y** Q P	7.0	1600	1619	
Peptide 561–575					[24]
561–572	I **S** N P **A A T H** Q **D** I D	5.0	1461	1524	
562–574	S N **P** A A **T** H **Q D** I **D** F L	"	1490	1543	
563–575	N P **A** A T **H** Q **D I** D **F** L I	7.0	1533	1514	
B4 Coxsackie virus, C-2 protein					[43]
32–47	L K **V** K I **L** P **E V** K **E** K H	5.0	1675	1637	
33–45	K V **K** I L **P** E **V K** E **K** H E	7.0	1639	1610	
Murine insulin					[44, 45]
B11–23	L V **E** A L **Y** L **V C** G **E** R G	5.0	1458	1464	
B12–24	V E **A** L Y **L** V **C G** E **R** G F	7.0	1573	1578	
Murine Ii (88–100)					[26]
CLIP	S Q **M** R M **A** T **P L** L **M** R P	5.0 or 7.0	1544	1501	
Murine serum albumin					[19, 26]
563–574	A T **A** E Q **L** K **T V** M **D** D	5.0	1413	1538	
Murine transferrin					[19, 26]
57–68	N Y **V** T A **I** R **N Q** Q **E** G	5.0	1400	1466	
55–65	**G** H N **Y** V **T A** I **R** N Q	7.0	1755	1721	
Murine MHC II peptides					[19, 25, 27]
I-A^{g7} β87–97	**V** P T **S** L **R R** L **E** Q P	5.0	1455	1434	
I-Eα 48–58	F A **K** F **A S** F **E** A Q	5.0	1623	1603	
I-Eα 54–68	F E **A** Q G **A** L **A N** I **A** V D K A	5.0	1500	1523	
I-Eα all Ala anchors	A E **A** A A **A** L **A A** I **A** A A A A	5.0	1541	1506	
Scrambled peptide[d]	V N **Q** S L **R** P **T P** L **E** I S	5.0	1449		
Human Carboxypeptidase H 362–382					[18, 26]
362–372	**K** N S **L** I **N Y** L **E** Q I	5.0	1468	1502	
369–381	L E **Q** I H **R** G **V K** G **F** V R	7.0	1634	1636	
Myoglobin					[46, 47]
Equine 69–78	L **T** A L **G G I** L **K K**	7.0	1633	1614	
Equine 69–78[e]	**L** T A **L** G **G I** L **K** K	"	1633	1599	
Mouse 69–78	L **T** A L **G** T **I** L **K K**	7.0	1671	1604	
Mouse 69–78[e]	**L** T A **L G T I** L **K** K	"	1633	1591	
Sperm whale 108–120	S E **A** I I **H** V **L H** S **R** H P	7.0	1901	1799	
Sperm whale 110–120	**A** I I **H** V **L H** S **R** H P	"	1728	1837	
Mouse 110–120	**I** I I **E** V **L K K R** H S	7.0	1856	1771	
Mouse 110–119	I I **I** E **V L K K R** H	"	1748	1587	

[a] References here denote sources where these peptides were shown to be antigenic. Reference 21 also contains a table aligning known immunogenic for the NOD mouse peptides in the register fulfilling the motif found by these workers (i. e. pH 5) and reference 22 makes extensive use of substitutions to verify its motif (pH 7)

[b] The HEL 10–22 peptide is the only one from the list above that has had characterisation of its binding affinities by extensive substitution at each position, as reported [22]

[c] Reference 38 tested peptide 221–235, in which only the 12-mer 221–232 could bind in the pH 7 motif register with 222K as p1 anchor and reference 40 tested the sequence 217–236 which contains the 217–227 11-mer with 217E as p1 anchor

[d] Control peptide for first two peptides in the series [25]

[e] Alternative register of same sequence

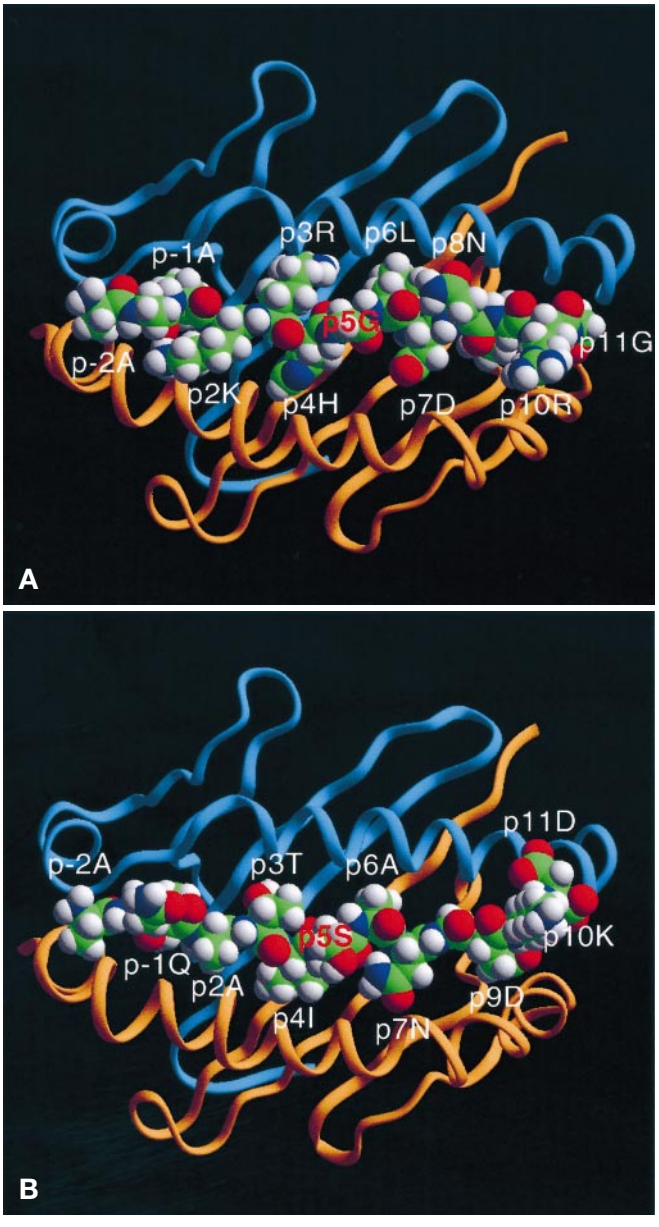

Fig. 2 A, B. Three-dimensional structure of the modelled α1β1 domain of I-A^{g7}, complexed (**A**) with the HEL10–22 peptide (p1 as 12Met) at pH 7 and (**B**) with the mouse hsp60 peptide 12 at pH 5 (alpha and beta chains in ribbon form) as viewed from "above" (T-cell receptor view). The α1 domain is in light blue, the β1 domain is in brick red and the antigenic peptide residues are in space-filling form. The orientation and hydrogen bonding distances were essentially the same for the various peptides modelled, regardless of the pH value. Carbon: green, oxygen: red, nitrogen: blue, hydrogen: white, sulphur: yellow

produced a reduction in total energy by about 2.5% with no cross-overs in the energy differences among the different complexes. The consistent valence force field of Discover was used, which included electrostatic terms for interactions up to 16 Å. A simple harmonic potential rather than a Morse potential was used and no cross-terms were included. The dielectric constant used was 1/r. No account was taken of the water molecules. The coordinates of the I-A^{g7} complexed to peptide 12 of hsp60 at pH 5, and to the HEL10–22 peptide at pH 7, will be deposited in the Protein Data Bank and in the meantime are available from the authors.

Table 2. Groups from α1β1 of I-A^{g7} that participate in hydrogen bonds to the antigenic peptide backbone[a]

I-A^{g7} group	Peptide backbone group	Equivalent hydrogen bond found in[b]	
		I-A^{k}	I-A^{d}
α51 N	p-2 NH	No	No
α53 N	p-2 O	Yes	Yes
β81His Nε2	p-1 O	Yes	Yes
α53 O	p1 NH	Yes	Yes
β82Asn Oδ1	p2 NH	Yes	Yes
β82Asn Nδ2	p2 O	Yes	Yes
α24His Nε2	p2 O	NA[c]	No
α9Tyr Oη	p4 NH	Yes	Yes
α62Asn Nδ2	p4 O	No	Yes
β74Glu Oε2	p5 NH	Yes	Yes
β70Arg Nη2	p5 O	No	No
α11Thr Oγ	p5 O	No	No
α62Asn Oδ1	p6 NH	Yes	Yes
β30Tyr Oη	p7 NH	Yes	Yes
α69Asn Nδ2	p7 O	Yes	Yes
β67Tyr Oη	p8 NH	No	NA[d]
β61Tyr Oη	p8 O	No[e]	Yes[e]
α69Asn Oδ1	p9 NH	Yes	Yes
α68His Nε2	p9 O	Yes	Yes

[a] No account is taken of hydrogen bonds between side-chains of the protein and the antigenic peptide
[b] Data obtained by inspection of the deposited coordinates
[c] Not applicable, I-A^{k} has a Phe at this position
[d] I-A^{d} has a Glu at this position
[e] I-A^{d} and I-A^{k} have a Trp at this position

Results

Overall structural features. We put 93 different peptide sequences in complex with I-A^{g7} through the energy minimisation process, at pH 5 or pH 7 or both for a total of 158 minimisations (Table 1). The resulting I-A^{g7} molecule, whether at pH 5 or at pH 7, shows very little deviation in its secondary, tertiary and quaternary structure from that of I-A^{k}. Figure 2 shows the overall shape of the α1β1 domain of the I-A^{g7} molecule in complex with peptide 12 of mouse hsp60 protein (at pH 5) and with HEL10–22 (at pH 7). Hydrogen bonds with the amide and carbonyl groups of the bound peptide are formed by the same or equivalent polar residues in the α1β1 domain as in I-A^{d} and I-A^{k} (Fig. 1, 2; Table 2). The orientation of the backbones of the antigenic peptides is nearly identical to that of HEL50–62 in I-A^{k}, i.e. they have a downward bend at the centre, because of β13Gly.

Energy minimisation. We first tested whether the minimisation procedure would reliably predict the better binding peptides as those resulting in lower to-

tal energies of I-A^{g7}-peptide complexes. Thus we did the minimisation of the I-A^{g7}-peptide complexes of HEL10–22 and hsp60 peptide 12 and several of their truncated or substituted variants (one deletion or substitution at a time) because quantitative and semi-quantitative results of in vitro binding studies respectively were available for comparison [21–23]. Only in 3 out of 12 cases the energy of the I-A^{g7}-hsp60 peptide 12 variant complex did not correlate with reported binding, or lack of, to I-A^{g7}: in p1E the energy was lower than that of the reference peptide-I-A^{g7} complex, instead of the expected higher value and in p6T and p6E, the energies were lower instead of slightly higher than that of the same reference value (Table 1; [21, 23]). Likewise, there was very good correlation in 19 out of 22 cases between the energies of the substituted and truncated HEL10–22 peptides with I-A^{g7} in the pH 7 register and the experimentally derived affinities to this allele (discordant peptides 11–22, 12–22 and 13–22, Table 1, [22]); a plot of total energy against log IC_{50} for the HEL peptides yielded a linear result (data not shown). We observed no statistically significant energy differences among different preferred residues in pockets 1, 4 and 7 between pH values of 5 and 7 (data not shown). Thus, any pH-dependent motif differences at these pockets are very small. A standard deviation of 5.2 kcal/mol was obtained from the repeated (ten times) minimisation, starting from a different atom each time, of the I-A^{g7}-HEL10–22 complex at pH 7. Therefore, we consider energy differences of ± 13.2 kcal/mol (± 2.54 SD) as significant ($p < 0.01$).

A comparison of energy values can be made for the same I-A^{g7}-peptide complex at two different pH values. Likewise, the deletion, addition or substitution of one residue to a peptide "bound" to I-A^{g7} can be compared with the "native" peptide bound in the same register. Comparisons of the minimised energy of different peptide-I-A^{g7} complexes, when the peptide sequences bear no relation to each other, have little meaning. Furthermore, as these minimisations do not consider possible interactions with water molecules, no correlation between the total energy of the various I-A^{g7}-peptide complexes and their respective dissociation constants can be made.

Table 1 shows the total energy values obtained for several I-A^{g7}–13mer antigenic peptide complexes. Within a 20-residue immunogen all possible pH 5 or 7 registers were tried, to obtain the corresponding minimised energy structures. In 36 out of 58 (62%) cases tried, the lower energy value (at pH 5 or pH 7) was obtained when a peptide was fitted into the groove in the register fulfilling the motif concordant with the ambient pH of the I-A^{g7} molecule ($p < 0.07$ by the chi-squared test). In 9 out of 58 (16%) cases the energy differences were non-significant and in 13 out of 58 (22%) cases they correlated with the discordant binding register.

The complexes of several established antigens with I-A^{g7} yielded minimised energy values that are mostly consistent with the existence of two pH-dependent motifs at p6 and p9 (Table 1). In particular, the four decamers/dodecamers from mouse and equine myoglobin [amino acids (aa) 69–78] and mouse and sperm whale myoglobin [aa 110–121] contained only pH 7 motif sequences (one or more) but not a single pH 5 motif sequence. In 7 out of 8 cases these complexes had significantly lower energies at pH 7 than at 5, also in agreement with the existence of pH-dependent motifs (Table 1). In the immunisation of NOD mice and in proliferation studies of primed lymph node T-cells with these peptides [46, 47], their binding to I-A^{g7} would not be through the endosome but at the cell membrane (ambient pH of 7.4). We conclude that the motifs already reported [21, 22], derived from binding and proliferation studies performed at specific pH values (5 or 7, respectively), generally reflect the respective preferences at pockets 6 and 9 at the given pH values, as shown by the majority of our energy calculations.

The shape of pocket 9 at endosomal and extracellular pH. Pocket 9 of the I-A^{g7} molecule is composed of residues α68His, α69Asn, α72Ile, α73Leu, α76Arg, β9His, β30Tyr, β37Tyr, β57Ser and β61Tyr (Fig. 1, 3). The substitution of β61Trp (near-universally conserved among MHC II alleles) for Tyr and the absence of a β57Asp make for a slightly more spacious p9 pocket compared to other I-A alleles. At the endosomal pH (5.0–5.5), this pocket contains three positively charged residues, β9His, α68 His and α76Arg and has another two positively charged residues, β55Arg and β56His, in its immediate vicinity (Fig. 3 A). Because of the extensive electrostatic repulsions in pocket 9 at pH 5, the oppositely positioned α76Arg and β57Ser are 2 Å further apart than at pH 7, when the groove is occupied by a peptide in the pH 7 motif register (Table 3). Our modelling showed that in all peptides fitted in the pH 5 motif register, the carboxyl group from a p9Asp/Glu would strongly interact with the α76Arg and less so with the β57Ser side-chains and thus not penetrate much into p9 (Fig. 3, Table 3). This arrangement would also counteract the electrostatic repulsions among these five positively charged residues of pocket 9. The distance between β9His and the terminal carboxylate from a p9Asp/Glu at pH 5 is 9–11 Å (Table 3). At endosomal pH water molecules would probably fill this space [14, 15]. Therefore, β9His would be exposed to solvent and become unprotonated at extracellular pH (see below).

At neutral pH there is only one positive charge in pocket 9, from α76Arg, and one close to it, that of β55Arg (Fig. 3 B). Thus, the interaction energy between the acidic residue at p9 and nearby positively charged residues of I-A^{g7} is considerably decreased

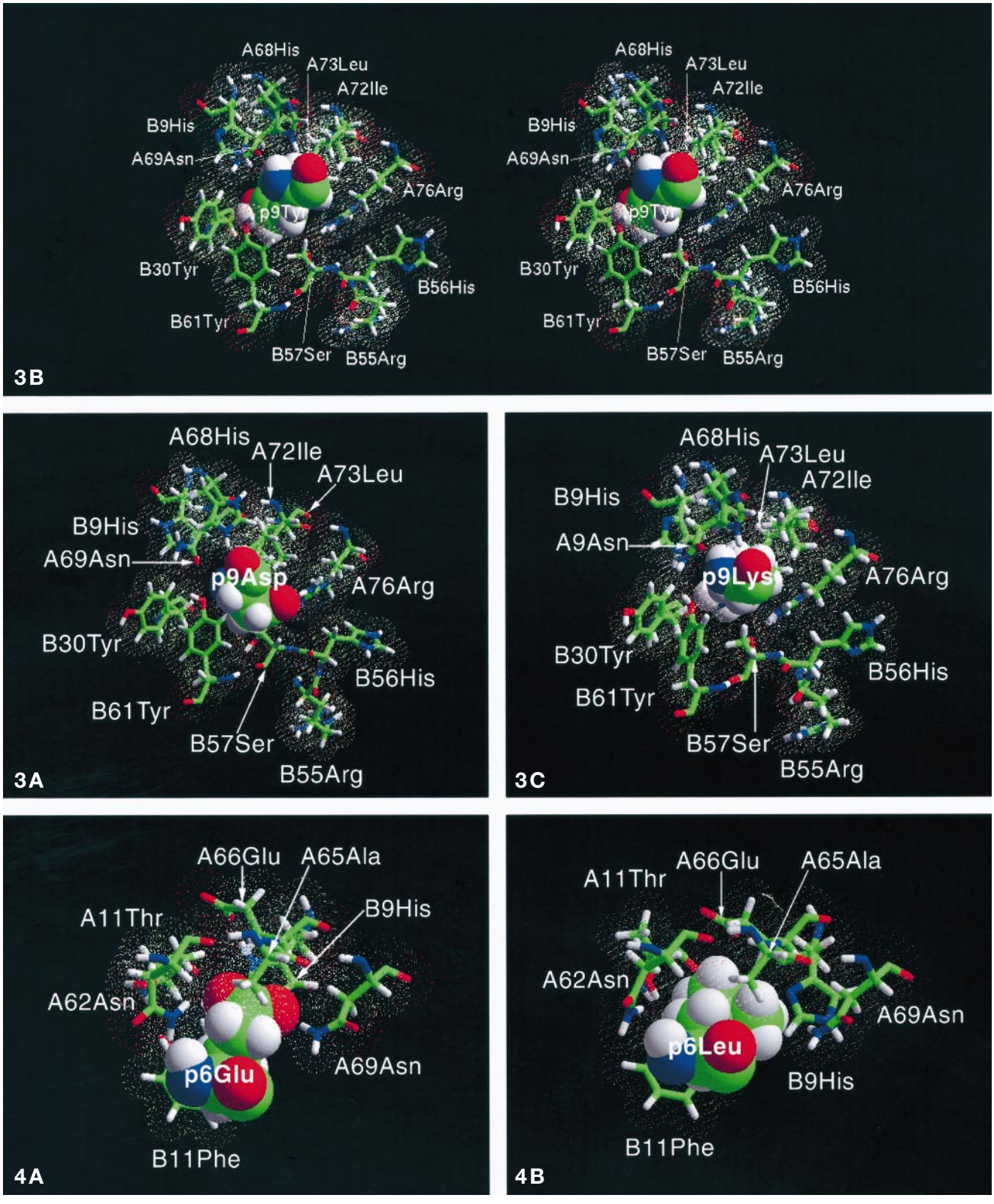

Fig. 3 A-C. The shape of pocket 9 seen in mono (**A**, **C**), or stereo (**B**) representation, with residue p9 in space filling mode and the residues from I-A^{g7} forming the pocket in stick and van der Waals dot surface representation. **A** At pH 5, containing the Asp residue of peptide 12 from murine hsp60. Residue β37Tyr is not shown, as it is mostly covered by residue p9 in the angle at which all three pictures of pocket 9 were taken. The orientation of acidic residues in p9 at pH 5 is essentially the same in all cases of antigenic peptides of Table 1 bearing such a residue. **B** At neutral pH with the Tyr20 residue of HEL. At endosomal pH, besides the positively charged histidines at α68, β9 and β56, there are also two positively charged arginines (α76 and β55). There is a distinctly different orientation of β55Arg and β56His at pH 7, because of the absence of electrostatic repulsions between β56His and β55Arg or α76Arg. At pH 7 the four preferred residues (Arg, Lys, Phe and Tyr) penetrate equally well into the p9 pocket, interacting with the proximal aromatic amino acids β30Tyr and β37Tyr by hydrogen bonding, π-cation, van der Waals and (in the case of Phe/Tyr) aromatic-aromatic, interaction mechanisms. **C** The fitting of p9Lys residue 534 from peptide 35 of mouse GAD65, i.e. from sequence 524–536, in pocket 9 at pH 7

Table 3. Distances (in Å) between various interacting atoms in pocket 9

Molecule	Residue/ Atom	α76Arg		β9Val		β9His		β30 Tyr Oη	β37Tyr Oη	β30Tyr	β37Tyr
		Nη1	Nη2	Cγ1[a]	Cγ2[a]	Nδ1[b]	Nε2[b]			Aromatic Cs	
I-A^d	β57Asp/Oδ1	3.17	3.35								
I-A^d	β57Asp/Oδ2	3.27	4.33								
I-A^d	p9Ala/Cβ			9.65	10.58						
I-A^k	β57Asp/Oδ1	3.84	3.01								
I-A^k	β57Asp/Oδ2	2.69	3.33								
I-A^k	p9Ser/Oγ					8.19	6.87				
I-A^{g7}-HEL10–22 (pH 7)	β57Ser/Oγ	2.94	3.86								
I-A^{g7}-HEL10–22 (pH 7)	p9Tyr/Oη					6.51	4.59	5.84	2.54		
I-A^{g7}-HEL10–22 (pH 7)	p9Tyr/aromatic Cs	4.66–5.03	4.09–5.32							4.42–8.25	3.71–8.16
I-A^{g7}-mGAD 524–536 (pH 7)	β57Ser/Oγ	2.85	3.84								
I-A^{g7}-mGAD 524–536 (pH 7)	p9Lys/Nζ						6.13			4.18–5.86	4.61–7.09
I-A^{g7}-hsp60 peptide 12 (pH 5)	β57Ser/Oγ	5.19	6.00								
I-A^{g7}-hsp60 peptide 12 (pH 5)	p9Asp/Oδ1	3.08	2.64			13.37	11.52				
I-A^{g7}-hsp60 peptide 12 (pH 5)	p9Asp/Oδ2	2.91	3.89			11.7	9.75				

Values for the distances between β57SerOγ and α76ArgNη1/Nη2, and β9HisNδ1/Nε2 and the terminal atoms of the p9 residue are typical of what is obtained after minimisation with peptides fitted in the pH 5 or the pH 7 register with the minimisation done at the concordant pH

Data of I-A^d are from 1iad.pdb, and of I-A^k from 1iak.pdb, whereas all the data for I-A^{g7}-peptide complexes are from our own energy minimisations as described in Materials and methods

[a] Refers to I-A^d only

[b] Refers to I-A^k and I-A^{g7} only

(Table 1). Modelling of the fit of the high affinity HEL10–22 peptide and several of its variants in the neutral pH register indicates that Phe/Arg/Lys also fit well in p9, yielding low total energy values whereas non-favoured residues show the opposite (Table 1). Note that with a p9Arg/Lys/Phe/Tyr there is deeper penetration into the p9 pocket, additional hydrogen bonds and many van der Waals contacts between such p9 residues and the various I-A^{g7} residues constituting the p9 pocket, in contrast to the situation at pH 5 with an acidic residue at p9 (Table 3).

We examined in detail the structure of p9 of I-A^{g7} at pH 7 for an explanation of the unique Arg/Lys/Phe/Tyr selectivity of this pocket [16]. The orientation of the positively charged end of a p9Arg/Lys in the models of I-A^{g7} at pH 7 allows maximum interaction with the aromatic ring of β37Tyr and less so of β30Tyr (Fig. 3C, Table 3). This situation is identical to the π-cation interactions observed with the aromatic amino acids Tyr/Phe/Trp and positively charged Arg/Lys residues that contribute greatly to the binding between the respective groups [49]. In addition, the aliphatic parts of α72Ile and α73Leu come in close contact with the aliphatic portions of the p9Arg/Lys side-chain, as well as the p9Phe/Tyr aromatic ring, thus increasing the van der Waals contacts and the stability of the complex. The binding of Phe/Tyr at p9 is also stabilised by a π-cation interaction between such residues and α76Arg, as the distances between the interacting groups indicate (Table 3).

Another possible contributory factor to the aromatic preference at p9 is the presence of an extensive interacting network of seven aromatic amino acids. The array of β11Phe, β30Tyr, β37Tyr, β47Tyr, β60Tyr, β61Tyr and β67Tyr would be further stabilised by the presence of a Phe/Tyr at p9. The centre of each of these aromatic residues is less than 7 Å away from at least one centre of another aromatic residue (Table 3, Fig. 3B), the cut-off distance for interactions of this type [50].

The interaction of the two crucial residues of pocket 9, α76Arg and β57Ser, is important to the stability of the MHC II-peptide complex [9–15]. In the crystal structures of I-A^k and I-A^d, both of which exhibit the β57Asp-α76Arg salt bridge at this interphase, the various interatomic distances between interacting groups are small. In I-A^{g7} at pH 7 with a Phe/Tyr/Arg/Lys occupying p9 the corresponding distances are increased by 15–40 % whereas at pH 5 and with an acidic residue in p9 the distances are further increased (Table 3). Thus, interactions at the p9 junction become progressively weaker from I-A^k/I-A^d to I-A^{g7} both at pH 7 and pH 5 because their energy is inversely proportional to the first and higher powers of the separating distances ([51], see Discussion).

The structure of pocket 6 at endosomal and extracellular pH. Pocket 6 of I-A^{g7} is bounded by α11Thr, α62Asn, α65Ala, α66Glu, α69Asn, β9His and β11Phe, of which α66Glu and β9His are ionisable. The crystal structures of I-A^d (β9Val) and I-A^k

Fig. 4 A, B. The shape of pocket 6 of I-A^{g7} at **A** pH 5, containing the 517Glu residue of mouse GAD65 peptide 34 (aa510–522) and **B** neutral pH containing the 17Leu residue of HEL10–22. Carbon: green, oxygen: red, nitrogen: blue, hydrogen: white, sulphur: yellow. Representations of antigenic and pocket residues as in Fig. 3

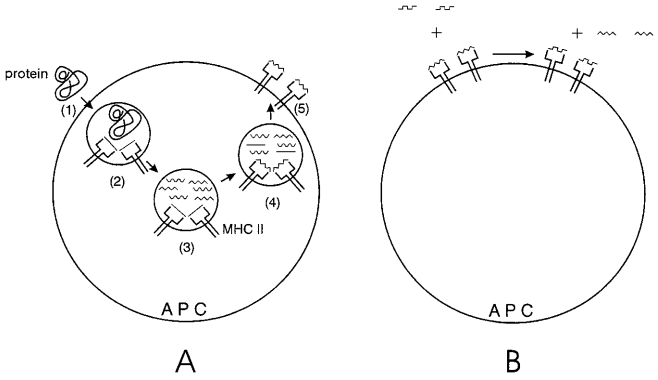

Fig. 5 A, B. Because I-A^{g7} is shown to have two different peptide-binding motifs, one at pH 5 and another at pH 7, that differ in their selectivity at p6 and p9, a difference in antigenicity could be evident between peptide and protein antigens. **A** Whole proteins are endocytosed by APCs (1), brought to the endosomal compartment (2), processed by proteolytic enzymes into peptides 15–22 residues long [16] (3); these peptides (⩙: Sawtooth, ⩛: Sineware), provided they fulfil the binding motif, are exchanged with CLIP (___) in the groove of MHC class II proteins at about pH 5–5.5 (part 4) and the complexes end up on the cell membrane (5), bathed by the extracellular medium with a pH of 7.4. The possibility of dissociation and rebinding is discussed in the text and shown in Fig. 6 for HEL8–22. Thus, epitopes arising from intracellularly processed proteins must satisfy the pH 5 motif to be loaded onto I-A^{g7} at the endosome, and the pH 7 motif to remain bound at the cell membrane, a condition mostly satisfied in different registers. **B** Free peptides (either injected into animals or given in vitro) that satisfy the pH 7 motif alone, can simply displace weakly bound peptides from I-A^{g7} at the cell surface [63], if they are themselves of higher affinity. This is probably best illustrated by the myoglobin nonamer and decamer peptides that contain only a pH 7 motif (Table 1)

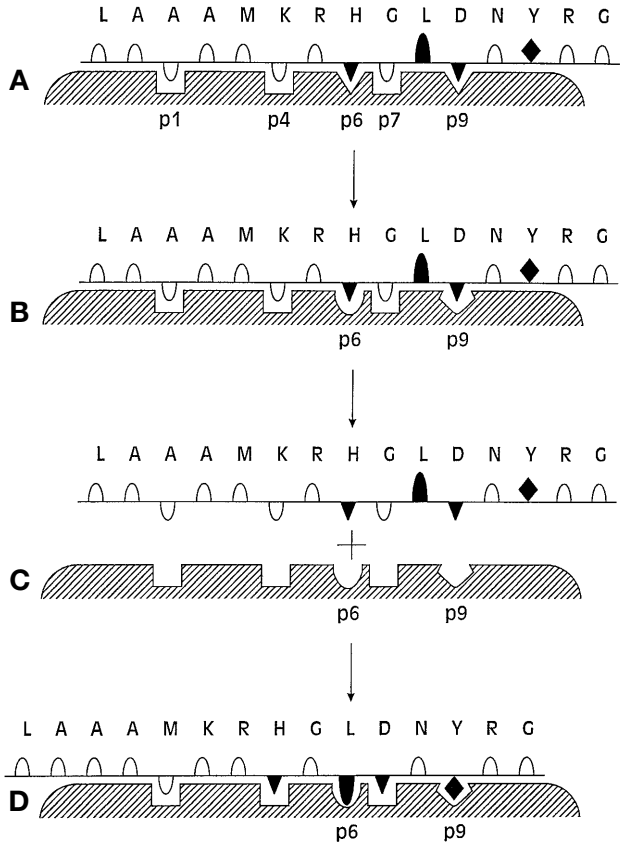

Fig. 6 A-D. The effect of pH-dependent motif changes on transition of the I-A^{g7} molecule from endosomal to extracellular pH. As pockets 1, 4, and 7 seem not to change in selectivity from one pH to the other, we depict them as indifferent (⌓) whereas pockets 6 and 9 accommodate mostly acidic residues at endosomal pH (▼). At extracellular pH pocket 6 prefers an aliphatic residue (▲) whereas pocket 9 accommodates aromatic or positively charged bulky residues (◆). The example depicted is that of HEL8–22 peptide. **A** Loading of HEL8–22 onto I-A^{g7} in the endosome with 15His at p6 and 18Asp at p9. **B** The change in pH (7.4) at the cell membrane, alters the architecture of pockets 6 and 9 that consist of one or more ionisable histidines (pK_a = 6.0). **C** As the HEL8–22 peptide does not fit well at pH 7 in this register, the peptide dissociates from I-A^{g7}. **D** The peptide can fit into the groove at pH 7 in a register shifted by two residues to the right, i.e. with 17Leu at p6 and 20Tyr at p9. There are few peptides with residues that show intermediate affinity at p6 and p9 both at pH 5 and pH 7 and fit well at p1, p4 and p7, which could remain attached to I-A^{g7} at pH 7 in the register bound at pH 5. Many more peptides loaded onto I-A^{g7} in the endosome do not fulfil the pH 7 motif, hence dissociate from this MHC II allele at the cell surface, leading to its observed instability in vivo. It is possible that the free peptide will exchange with a complex as in **B** because this conformation of I-A^{g7} is receptive for higher affinity binding [63]

(β9His) show the β9 residue to be part of pocket 6 as well as pocket 9 [14, 15]. Likewise, our modelling shows that β9His of I-A^{g7} also participates in the formation of pocket 6 and interacts with the p6 residue. In particular, at pH 5 the positively charged β9His interacts with the negatively charged α66Glu (Fig. 4 A), an interaction that probably determines the selectivity at p6, i.e. acidic/polar residues (Table 1). By contrast, at pH 7, the now uncharged β9His turns away from α66Glu and towards α76Arg (Fig. 4 B). Thus, at pH 7 pocket 6 would no longer favour the binding of acidic residues. Instead, aliphatic residues could interact well with α11Thr, α65Ala and β11Phe and are therefore favoured as shown from the energy minimisation studies (Table 1, Fig. 4 B).

Discussion

We have presented a structural modelling analysis of the pH-dependence of the binding preferences at pockets 6 and 9 of I-A^{g7}, the unique MHC class II molecule of NOD mice and chief genetic component of Type I diabetes in this model [1–3]. Homology modelling methods for prediction of protein structure are usually very successful when the modelled and the base protein have a greater than 40% amino acid identity and similar biochemical function [52]. The HIV-1 protease has been successfully modelled

Table 4. Comparison of residue preferences at various pockets at pH 5 and 7[a]

Binding character of residue at each pocket	p1		p4		p6		p7		p9	
	pH 5	pH 7	pH 5	pH 7	pH 5	pH 7	pH 5	pH 7	pH 5	pH 7
wl.t.[b]	A,E,K, L,Q,T, Y	A,D,K, L,M,Q, Y	A,L,Y	A,H,K, L,Q,Y	A,E,T	I,L,M, V	L,R	A,D,E, K,L,P, Q,R,Y	A,E	F,K,R, Y
wk.t.[b]	R	P	K,Q,T	D,P	K,L,Q, Y	D,F,H, K,N,T, Y	A,K		K,L,M, Q,T	D,H,L, M,N,Q, W
n.t.[b]			E			A,E,G, P,Q,R, S,W			Y	A,E,G, I,P,S, T,V

[a] Data from references 21 and 22, with permission from the authors and the publishers

[b] wl.t.: well tolerated (IC_{50} < 1 μmol/l), wk.t.: weakly tolerated (IC_{50} = 1–10 μmol/l), n.t.: not tolerated (IC_{50} > 10 μmol/l) for binding to purified I-A^{g7} (pH 7 motif, [22]). For motif testing by competitive peptide binding and proliferation of a T cell line (pH 5 motif, [21]): wl.t.: residues causing ≥ 50 % inhibition, wk.t.: causing 10–50 % inhibition, n.t.: causing < 10 % inhibition

Table 5. Consideration of binding of polyalanine peptide and HEL10–22 variants to I-A^{g7} in a different register

Alignment of reference 22	IC_{50} (nmol/l)[a]	Alternative alignment shifted by two positions to the left[b]
Anchor position: **1 4 6 9**		**1 4 6 9**
K**A**A**L**A**Y**A	50	K**A**AA**L**A**Y**A
AA**A**A**L**A**Y**A	50	A**A**AA**L**A**Y**A
AAAA**L**A**Y**	25	AA**A**AA**L**A**Y**
AA**A**A**L**A**Y**	200	A**A**AA**L**A**Y**
AAA**M**KR**H**G**L**D**NY**RG	300	AAAMK**R**HG**L**D**NY**R**G**
AAA**M**KR**H**G**L**D**NY**R	300	AAAMK**R**HG**L**D**NY**R
AAA**M**KR**H**G**L**D**NY**	150	AAAMK**R**HG**L**D**NY**
AAA**M**KR**H**G**L**DN	15,000	AAAMK**R**HG**L**DN

Putative anchors at p1, p4, p6, p7 and p9 in bold

[a] As reported in [22] for binding to purified I-A^{g7} at pH 7.0, after permission from the publisher and authors

[b] Alignment arising as suggested [60] to explain the data of reference 22

on its Rous Sarcoma Virus acid protease relative while having only 33 % amino acid identity. Furthermore, this modelling was sufficiently accurate around the active site of the HIV-1 protease (where homology to acid proteases was even higher), to allow for the designing of very potent inhibitors to the enzyme [52]. The identity between I-A^{g7} and the base protein I-A^{k} is more than 87 % in any domain, thus the modelled structures obtained should be highly similar to the actual ones, particularly as these two molecules share the crucial β65–66 deletion. Peptide binding and homology modelling studies of mouse and human MHC class II proteins have shown results consistent with the view that HLA-DQ and I-A alleles resemble very much the fold shown in the crystal structures of the homologous (55–65 % identity) proteins HLA-DR and I-E [53–57]. These studies also explain well the selective binding of given residues from antigenic peptides to specific pockets of the HLA-DQ/DR and I-A/I-E molecules, such as the exclusion of acidic residues from p4 of DRB1*0402 [12], the preferences for acidic residues at p4/p7 and tryptophan at p9 of DQ2 [55, 56] and for acidic residues at p1 of I-A^{k} [57] and at p4 of I-E^{g7} [58].

Our energy calculations, like all other modelling studies, do not consider bound water molecules. Water molecules act as hydrogen bond bridges between the antigenic peptide backbone and the MHC II protein [11, 14]. Use of water molecules in the minimisation process did not seem feasible in the program used. The use of version 97 of the QUANTA-CHARm program (MSI, San Diego, Calif., USA) allowed us to place ten layers of water molecules over the antigen binding groove of HLA-DR1, obtaining better agreement with experimental data for the binding of peptides to DR1 (Papandreou, van Endert, Eliopoulos and Papadopoulos, unpublished results). There still is, however, no reliable approach for treating the interactions of water molecules with MHC-peptide complexes.

The allele-specific motif of I-A^{g7} has the remarkable property of different specificities at neutral and

endosomal pH, at pockets 6 and 9, as also reported from two previous independent experimental studies [21, 22]. Our modelling studies, with practically all established antigenic peptides of the NOD mouse in complex with I-A^{g7}, verify the pH selectivity of p6 and p9 of this MHC class II allele as manifested in the lower energy values of most complexes with I-A^{g7} in the concordant register ($p < 0.07$). For the peptides showing lower minimised energy at the discordant pH, or no significant energy difference between the two pH values, there could be other contributory factors to such binding, e.g. favourable interactions at the other pockets and interactions of particular "upward-pointing" peptide residues with amino acids of I-A^{g7} (haemagglutinin p5His to α61Gln of I-A^{d}, HEL53Tyr to water I-A^{k} etc., [14–15]). Our physicochemical analysis attributes this unique selectivity at p6 and p9 to the combination of β9His, β56His and β57Ser. No other MHC II allele has more than one of these three substitutions [6, 7]. The histidine residues in pockets 6 and 9 are positively charged at pH 5 and uncharged at pH 7, altering considerably the preferences at these two pockets. In particular, β9His is found pointing towards α66Glu at pH 5 and towards α76Arg at pH 7 (Fig. 4). This flipping of β9His by 180° has also been considered for I-A^{k} [14].

These pH-dependent changes in residue selectivity at specific pockets have not been reported for any MHC class II allele, in contrast to differences in peptide affinity at pH 5 and 7 [59]. The latter concern pH-sensitive interactions of the peptide backbone with select MHC II residues [11]. The possibility of misalignment of the registers by either of the two I-A^{g7} motif studies (e.g. preferences at p9 and p6 of [22] match those at p7 and p4, respectively of [21]), as suggested [60], is ruled out by three considerations.

Firstly, there is general agreement about the preferred residues in pockets 1, 4 and 7 (Table 4). Secondly, although a shift by two positions to the left would match some of the preferences, it would contradict several others (Table 4). Thirdly, a shifting of the binding register of the pH 7 motif by two positions to the left would leave some of the truncated peptide variants of HEL10–22 and the polyalanine-substituted peptides in the pH 7 binding studies without any residues at p8 and p9, despite their high affinity (IC_{50} values from 25 to 300 nmol/l), a highly unlikely possibility, not reported for any MHC class II allele thus far (Table 5).

Consistent with the above, when decamer/endecamer peptides from HEL10–22 were tested for binding to purified I-A^{g7} molecules at pH 7, only the sequences 12–21 and 12–20, that fulfil the pH 7 motif, bound to I-A^{g7} (IC_{50} of 1.00 and 1.25 μmol/l, respectively; [22]). The sequence 9–18 that contains only the pH 5 motif would not bind at all (IC_{50} equal to or greater than 15 μmol/l, respectively; [22]). These results are consistent with our own energy calculations. Additionally, the same group has found that a HEL10–22-specific, I-A^{g7}-restricted T-cell hybridoma responded only to the presence of the HEL12–21 peptide (p10 residue is necessary for T-cell recognition [22]) and not to the HEL9–18 or 9–19 peptides [22]. In a previous study [28], immunisation of NOD mice with intact HEL resulted in sensitised T-cells that would proliferate to many overlapping HEL peptides containing the pH 7 motif (aa12–20) but to none containing only the pH 5 motif (aa10–18). As the peptide in such proliferation assays is added exogenously (pH 7.4), the above results are strong evidence that at extracellular pH the HEL10–22 peptide binds to I-A^{g7} in one register only: with 12Met as its p1 anchor and 20Tyr its p9 anchor, i.e. fulfilling the pH 7 motif but not at all the pH 5 motif, as has been shown by us here. Furthermore, the fast that the immunogenic 69–78 and 110–120 myoglobin peptides have no pH 5 motif within their sequences but at least two pH 7 motifs, is additional evidence that the pH 7 motif is the one used by free peptides binding to I-A^{g7} on APCs in vivo and in vitro at extracellular pH.

In view of our results, three other binding studies deserve comment. In the first two, the proliferation of two different I-Eα52–68-specific and I-A^{g7}-restricted T-cell hybridomas was tested by having the mouse albumin peptide and its variants [19], or the native I-Eα peptide and its variants [27], compete for binding to cognate APCs, at extracellular pH. The first of these established a requirement for acidic residues at the peptide's carboxy-terminus [19]. The second found that a peptide containing the T-cell contact residues and a backbone of alanines bound to I-A^{g7} and stimulated the T-cells. This latter peptide shows lower total energy at pH 7 according to our calculations (Table 1). Because at pH 7 our results allow for p9Asp in some peptides and Ala is tolerated in nearly all pockets except p6 at the same pH, the conclusions of these two studies are not at variance with what is shown here. In the third study, the binding of various peptides to purified I-A^{g7} at pH 5 and 7.4 was tested, as well as the selectivity of the allele for various residues at p9 [26]. The results at pH 5 are in agreement with previous studies [19, 21, 23] showing preference for an acidic residue at p9 and with our energy calculations regarding the murine CLIP, serum albumin and transferrin peptides. However, in the competitive binding studies to I-A^{g7} at pH 7.4, the competitor peptide was used at about 5% saturation, making the drawing of any conclusions difficult.

Two modelling studies of I-A^{g7}, both based on the structure of DR1, were published [20, 21] before the pH 7 motif [22] was available. In one [21] β57Ser interacted with the p9 acidic residue whereas β56His pointed into the solvent and was considered as non-participating in the selectivity of pocket 9. In the other [20], modelling of I-A^{g7} showed a fitting for two antigenic peptides into the groove without testing for

particular residue preferences at p6 and p9. Our previous modelling study based on DR1, using the pH 5 and pH 7 motifs [48], found results similar to these reported here, yet certain interchain interactions were missed. Also certain structural features of I-A molecules, such as the β-bulge at α9a and the β84a insertion [14, 15], were not known at the time of these studies.

Our results indicate that the I-A^{g7}-peptide complexes at pH 5 with the peptide in the pH 5 motif register have greater interatomic distances at the crucial p9 junction of α76Arg-β57Ser, than corresponding complexes at pH 7 (Table 3). The importance of the p9 α76Arg-β57Asp junction to the peptide affinity of MHC class II alleles has been shown repeatedly [9–13, 16, 61]. As the interaction energies depend on 1/r (for charged groups), $1/r^2$ (for charged-polar group interactions), and $1/r^3$ (for polar group interactions), r being the distance between interacting groups, the increased distances would result in lower interaction energies and thus lower affinity, for I-A^{g7}-peptide complexes at endosomal pH (typical energy values for these interactions in closely spaced groups are 60, 3.6 and 0.5 kcal/mol, respectively [51]). Therefore the shorter distances between various residues around p9 at pH 7 would strengthen these interactions, leading to higher affinity binding. This conclusion is consistent with the results reported in the literature. Specifically, four binding studies at pH 4.5 to 5.5 showed binding curves with deduced dissociation constant (K_d) values of I-A^{g7} for various peptide antigens in the range of 2 to well over 100 μmol/l (except the albumin peptide K_d of about 100 nmol/l) [18, 24–26]. Of the two binding studies done at pH 7/7.4, one reported IC_{50} values leading to K_ds for native and synthetic peptide antigens ranging from 0.05 to 30 μmol/l [22] but in the other study such values, albeit for different peptides, were in the low to middle μmol/l range [26]. Even then, the interaction of I-A^{g7} with certain antigenic peptides could be weak. For example, the activation of three I-A^{g7}-restricted T-cell hybridomas and a T-cell line, each specific for a different antigen required the continuous presence of the antigen [18, 26]. There was no such requirement in an I-A^{k}-restricted hybridoma [18]. The T-cell activation was achieved in such cases because the required serial triggering of T-cell receptors after recognition of peptide-MHC complexes is accomplished even when the free peptide concentration is well below the IC_{50} value for binding of the peptide to the MHC protein [18, 22, 26, 62].

The majority of peptide-I-A^{g7} complexes have lower energies when in the concordant pH motif register, which means that such peptides derived from endocytosed proteins in the endosome of APCs would probably dissociate at the cell surface (pH 7.4). If the peptide fulfils within its processed length a pH 7 motif, it is possible to rebind in the latter register. We consider it noteworthy that all peptide epitopes arising from immunisation of NOD mice with whole proteins contain both a pH 5 and a pH 7 motif within their naturally processed length [63] (Fig. 5 and 6). This is not the case for peptide immunisation, as exemplified by the myoglobin peptides (Table 1).

Because of the lower concentration of dissociated peptide in extracellular space compared with that in the endosomal compartment, the percentage of such newly formed I-A^{g7}-peptide complexes would be low. Thus, there would be a rapid turnover of I-A^{g7} molecules at the cell surface. In addition, the I-A^{g7}-peptide complexes are of lower affinity due to weaker p9 interactions compared with β56Proβ57Asp^{+} alleles. Consequently, I-A^{g7} would be unstable to SDS treatment in vivo [18, 28–31] and in vitro [18, 26]. Such stability does not always correlate with high-affinity peptide binding [64] but in general this is considered to be the case [65]. From this viewpoint, our documentation of weaker expected affinities of I-A^{g7} to peptides is consistent with the instability of this allele to SDS. Only one laboratory has shown SDS-stability of such complexes [21, 23], a discrepancy possibly arising from the different procedure used by this group; specifically, the incubation of the immunoprecipitated I-A^{g7} molecules with the high affinity hsp60 peptide 12 at a high final concentration (200 μmol/l) at pH 5, before SDS treatment. This procedure would lead to SDS-stable complexes.

The existence of a pH 5 and a pH 7 motif for p6 and p9 of I-A^{g7} (as shown by us here) and the low to medium affinity with which this allele generally binds to peptides at either pH, lead to pH-dependent differences in peptide affinity, possible dissociation and probable rebinding in a different register and to low apparent stability at the cell membrane. Because of such unique properties there would be relatively few high affinity I-A^{g7}-peptide combinations that would result in negative selection in the thymus. The latter process would operate in NOD mice at a much higher threshold of peptide affinity than it does in most other mouse strains. Therefore, the NOD mouse would have a higher than normal number of positively selected I-A^{g7}-restricted autoreactive CD4^{+} T-cells emerging from the thymus. This hypothesis has already been put forth to explain experimental findings in NOD mice [46, 66] and further evidence has been provided by another laboratory [67].

The results of our modelling also provide a possible explanation of the protection from diabetes of NOD mice transgenically expressing modified I-A^{g7} or other MHC class II alleles [2, 4, 24, 68]. In all such cases the transgenically expressed MHC II molecule has a pH-invariant motif, with a higher peptide affinity and MHC II-peptide stability, due to the absence of β56His or presence of β57Asp or both. The transgenically expressed MHC II allele could eliminate or suppress the generation of diabetogenic CD4^{+} T-cells

by "determinant capture" or "repertoire skewing" or any other regulatory mechanism(s) [2, 24, 28, 68–72]. Such mechanisms have been shown in NOD mice to depend on the ratio of transgene/I-A^{g7} expression on APCs in the thymus and the periphery [36, 68–70].

In extrapolating our results to human Type I diabetes, it should be kept in mind that in humans the role of the β57 residue along with other subtle points in the structure of susceptible and resistant HLA-DQ alleles is paramount [2, 8, 57, 73], as the β9His-β56His-β57Ser combination is unique to I-A^{g7}.

Acknowledgements. G. K. Papadopoulos dedicates this work to his doctoral adviser, Professor Joseph Y. Cassim, Emeritus, of the Doctoral Program in Biophysics and the Department of Microbiology at The Ohio State University, Columbus, Ohio, USA, for teaching him the importance of structure to biological function.

This work was supported in part by a Biotech grant to G. K. Papadopoulos from the European Union (contract no. BIO4 CT95 0263) and a supplementary grant from the Hellenic Secretariat of Research and Technology. G. K. Papadopoulos wishes to thank Dr. E. Eliopoulos for his invaluable help in teaching him the fundamentals of the Silicon Graphics Indy workstation as well as the Biosym/MSI software. We also wish to thank Dr. H.-G. Rammensee for unpublished information that confirmed our insights into I-A^{g7}, and Dr. C. Bartsocas for his encouragement and support.

This work was presented in part at the 5th Biannual Meeting of the Hellenic Diabetes Association, Athens, March 1997 and the 34th Meeting of the European Association for the Study of Diabetes, Barcelona, Spain, September 1998 [ref. 48].

Note Added in proof: Very recent binding studies to I-A^{97} at pH 6 via phage display libraries have shown the pH 7 motif to be the predominant one [74]. Also, "empty" MHC class II molecules have been demonstrated on the cell membrane of mouse immature dendritic cells [75]; this, in concert with newly found extracellular proteolytic activities from such cells, raise new possibilities for antigen presentation in immune responses.

References

1. Kikutani H, Makino S (1992) The murine autoimmune diabetes model: NOD and related strains. Adv Immunol 51: 285–322
2. Tisch R, McDevitt H (1996) Insulin-dependent diabetes mellitus. Cell 85: 291–297
3. Wicker LS, Todd JA, Peterson LB (1995) Genetic control of autoimmune diabetes in the NOD mouse. Annu Rev Immunol 13: 179–200
4. Nishimoto H, Kikutani H, Yamamura K-i, Kishimoto T (1987) Prevention of autoimmune insulitis by expression of I-E molecules in NOD mice. Nature 328: 432–434
5. Acha-Orbea H, McDevitt HO (1987) The first external domain of the nonobese diabetic mouse class II I-A β chain is unique. Proc Natl Acad Sci USA 84: 2435–2439
6. Kabat EA, Wu TT, Reid-Miller M, Perry HM, Gottesman KS (1991) Aminoacid sequences of proteins of immunological interest, (5th edn). NIH, Bethesda
7. Marsh SGE (1998) HLA Class II region sequences, 1998. Tissue Antigens 51: 467–507 (Also at the net site http://www.anthonynolan.org.uk/HIG/)
8. Todd JA, Bell JI, McDevitt HO (1987) HLA-DQ$_\beta$ gene contributes to susceptibility and resistance to insulin-dependent diabetes mellitus. Nature 329: 599–604
9. Stern LJ, Brown JH, Jardetzky TS, Gorga JC, Urban RG, Strominger JL, Wiley DC (1994) Crystal structure of the human class II MHC protein HLA-DR1 complexed with an influenza virus peptide. Nature 368: 215–221
10. Ghosh P, Amaya M, Mellins E, Wiley DC (1995) The structure of an intermediate in class II MHC maturation: CLIP bound to HLA-DR3. Nature 378: 457–462
11. Fremont DH, Hendrickson WA, Marrack P, Kappler J (1996) Structures of an MHC Class II molecule with covalently bound single peptides. Science 272: 1001–1004
12. Dessen A, Lawrence CM, Cupo S, Zaller DM, Wiley DC (1997) X-ray crystal structure of HLA-DR4 (DRA*0101, DRB1*0401) complexed with a peptide from human collagen II. Immunity 7: 473–481
13. Smith KJ, Pyrdol J, Gauthier L, Wiley DC, Wucherpfennig KW (1998) Crystal structure of HLA-DR2 (DRA*0101, DRB1*1501) complexed with a peptide from human myelin basic protein. J Exp Med 188: 1511–1520
14. Fremont DH, Monnaie D, Nelson CA, Hendrickson WA, Unanue ER (1998) Crystal structure of I-A^k in complex with a dominant epitope of lysozyme. Immunity 8: 305–317
15. Scott CA, Peterson PA, Teyton L, Wilson IA (1998) Crystal structures of two I-A^d-peptide complexes reveal that high affinity can be achieved without large anchor residues. Immunity 8: 319–329
16. Rammensee H-G, Friede T, Stevanovic S (1995) MHC ligands and peptide motifs: first listing. Immunogenetics 41: 178–228 (Also at the net site: http://www.uni-tuebingen/de/uni/kxi/)
17. Klein J (1986) Natural history of the major histocompatibility complex. John Wiley, New York
18. Carrasco-Marin E, Shimizu J, Kanagawa O, Unanue ER (1996) The class II MHC I-A^{g7} molecules from non-obese diabetic mice are poor peptide binders. J Immunol 156: 450–458
19. Reich E-P, von Grafenstein H, Barlow A, Swenson KE, Williams K, Janeway CA Jr (1994) Self peptides isolated from MHC glycoproteins of non-obese diabetic mice. J Immunol 152: 2279–2288
20. Amor S, O'Neill JK, Morris MM et al. (1996) Encephalitogenic epitopes of myelin basic protein, proteolipid protein, and myelin oligodendrocyte glycoprotein for experimental allergic encephalomyelitis induction in Biozzi ABH (H-2A^{g7}) mice share an aminoacid motif. J Immunol 156: 3000–3008
21. Reizis B, Eisenstein M, Bockova J et al. (1997) Molecular characterization of the diabetes-associated mouse MHC class II protein, I-A^{g7}. Int Immunol 9: 43–51
22. Harrison LC, Honeyman MC, Trembleau S, et al. (1997) A peptide binding motif for I-A^{g7}, the class II Major Histocompatibility Complex (MHC) molecule of NOD and Biozzi AB/H mice. J Exp Med 185: 1013–1021
23. Reizis B, Altmann DM, Cohen IR (1997) Biochemical characterization of the human diabetes-associated HLA-DQ8 allelic product: similarity to the major histocompatibility complex class II I-A^{g7} protein of non-obese diabetic mice. Eur J Immunol 27: 2478–2483
24. Chao C-C, Sytwu H-K, Chen EL, Toma J, McDevitt HO (1999) The role of MHC class II molecules in susceptibility to type I diabetes: Identification of peptide epitopes and characterization of the T cell repertoire. Proc Natl Acad Sci USA 96: 9299–9304
25. Xu X-J, Gearon C, Stevens E, Vergani D, Baum H, Peakman M (1999) Spontaneous T-cell proliferation in the non-

obese diabetic mouse to a peptide from the unique class II MHC molecule, I-A^{g7}, which is also protective against the development of autoimmune diabetes. Diabetologia 42: 560–565
26. Hausmann DHF, Yu B, Hausmann S, Wucherpfennig KW (1999) pH-dependent peptide binding properties of the type I diabetes-associated I-A^{g7} molecule: rapid release of CLIP at an endosomal pH. J Exp Med 189: 1723–1733
27. Carrasco-Marin E, Kanagawa O, Unanue ER (1999) The lack of consensus for I-A^{g7}-peptide binding motifs: Is there a requirement for anchor amino acid side chains? Proc Natl Acad Sci USA 96: 8621–8626
28. Deng H, Apple R, Clare-Salzler M et al. (1993) Determinant capture as a possible mechanism of protection afforded by major histocompatibility complex class II molecules in autoimmune disease. J Exp Med 178: 1675–1680
29. Carrasco-Marin E, Kanagawa O, Unanue ER (1997) Insights into the chemistry and biology of the I-A^{g7} class II molecule. Res Immunol 148: 291–301
30. Nabavieh A, Chou H, Volokhov I et al. (1998) Development of an I-A^{g7}-expressing antigen-presenting cell line: intrinsic molecular defect in compact I-A^{g7} dimer generation. J Autoimmun 11: 63–71
31. Peterson M, Sant AJ (1998) The inability of the nonobese diabetic class II molecule to form stable peptide complexes does not reflect a failure to interact productively with DM. J Immunol 161: 2961–2967
32. Baekkeskov S, Aanstoot H-J, Christgau S et al. (1990) Identification of the 64K autoantigen in insulin-dependent diabetes as the GABA-synthesizing enzyme glutamic acid decarboxylase. Nature 345: 151–156
33. Kaufman DL, Clare-Salzler M, Tian J et al. (1993) Spontaneous loss of T-cell tolerance to glutamic acid decarboxylase in murine insulin-dependent diabetes. Nature 366: 69–72
34. Tisch R, Yang X-D, Singer SM, Liblau RS, Fugger L, McDevitt HO (1993) Immune response to glutamic acid decarboxylase correlates with insulitis in non-obese diabetic mice. Nature 366: 72–75
35. Chen S-L, Whitley PJ, Freed DC, Rothbard JB, Peterson LB, Wicker LS (1994) Responses of NOD congenic mice to a glutamic acid decarboxylase-derived peptide. J Autoimmun 7: 635–641
36. Hanson MS, Cetkovic-Cvrlje M, Ramiya VK et al. (1996) Quantitative thresholds of MHC class II I-E expressed on hemopoietically-derived antigen-presenting cells in transgenic NOD/Lt mice determine level of diabetes resistance and indicate mechanism of protection. J Immunol 157: 1279–1287
37. Quinn A, Sercarz EE (1996) T cells with multiple fine specificities are used by non-obese diabetic (NOD) mice in response to GAD(524–543). J Autoimmun 9: 365–370
38. Chao C-C, McDevitt HO (1997) Identification of immunogenic epitopes of GAD 65 presented by A^{g7} in non-obese diabetic mice. Immunogenetics 46: 29–34
39. Cetkovic-Cvrlje M, Gerling IC, Muir A, Atkinson MA, Elliott JF, Leiter EH (1998) Retardation or acceleration of diabetes in NOD/Lt mice mediated by intrathymic administration of candidate β-cell antigens. Diabetes 46: 1975–1982
40. Zechel MA, Elliott JF, Atkinson MA, Singh B (1998) Characterization of novel T-cell epitopes on 65 kDa and 67 kDa glutamic acid decarboxylase relevant in autoimmune responses in NOD mice. J Autoimmun 11: 50–62
41. Boyton RJ, Lohmann T, Londei M et al. (1998) Glutamic acid decarboxylase T lymphocyte responses associated with susceptibility or resistance to type 1 diabetes: analysis in disease discordant human twins, non-obese diabetic mice and HLA-DQ transgenic mice. Int Immunol 10: 1765–1776
42. Tisch R, Wang B, Serreze DV (1999) Induction of glutamic acid decarboxylase 65-specific Th2 cells and suppression of autoimmune diabetes at late stages of disease is epitope dependent. J Immunol 163: 1178–1187
43. Tian J, Lehmann PV, Kaufman DL (1994) T cell cross-reactivity between Coxsackievirus and glutamate decarboxylase is associated with a murine diabetes susceptibility allele. J Exp Med 180: 1979–1984
44. Daniel D, Gill RG, Schloot N, Wegmann DR (1995) Epitope specificity, cytokine production profile and diabetogenic activity of insulin-specific T cell clones isolated from NOD mice. Eur J Immunol 25: 1056–1062
45. Zekzer D, Worg FS, Wen L et al. (1997) Inhibition of diabetes by an insulin-reactive CD4 T-cell clone in the non-obese diabetic mouse. Diabetes 46: 1124–1132
46. Ridgway WM, Fassò M, Lanctot A, Garvey C, Fathman CG (1996) Breaking self-tolerance in nonobese diabetic mice. J Exp Med 183: 1657–1662
47. Ridgway WM, Fathman CG (1998) The association of MHC with autoimmune diseases: understanding the pathogenesis of autoimmune diabetes. Clin Immunol Immunopathol 86: 3–10
48. Papadopoulos GK (1998) Homology modeling of I-A^{g7} verifies the existence of two peptide binding motifs (pH 5 and pH 7) explains several properties of this MHC II allele from NOD mice. Diabetologia 56: 101A (Abstract)
49. Dougherty DA (1996) Cation-π interactions in chemistry and biology: a new view of benzene, Phe, Tyr and Trp. Science 271: 163–168
50. Burley SK, Petsko GA (1985) Aromatic-aromatic interaction: a mechanism of protein structure stabilization. Science 229: 23–28
51. Atkins PW (1998) The Elements of Physical Chemistry, (2nd edn). Oxford University Press, Oxford, pp 377–378
52. Weber IT (1991) Modeling of structure of Human Immunodeficiency Virus-1 protease with substrate based on crystal structure of Rous Sarcoma Virus protease. Methods Enzymol 202: 727–741
53. Sanjeevi CB, Lybrand TP, DeWesee C et al. (1995) Polymorphic amino acid variations in HLA-DQ are associated with systematic physical property changes and occurrence of IDDM. Diabetes 44: 125–131
54. Paliakasis K, Routsias J, Petratos K, Ouzounis C, Kokkinidis M, Papadopoulos GK (1996) Novel structural features of the human histocompatibility molecules HLA-DQ as revealed by modeling based on the published structure of the related molecule HLA-DR1. J Struct Biol 117: 145–163
55. Vartdal F, Johansen BH, Friede T et al. (1996) The peptide binding motif of the disease associated HLA-DQ (α1*0501, β1*0201) molecule. Eur J Immunol 26: 2764–2772
56. van de Wal Y, Kooy YMC, Drijfhout JW, Amons R, Papadopoulos GK, Koning F (1997) Peptide-binding features of the disease-associated DQ(α1*0501,β1*0201) molecule versus the non-disease-associated DQ(α1*0201,β1*0202) allele. Immunogenetics 46: 484–492
57. Nelson CA, Viner NJ, Young SP, Petzol SJ, Unanue ER (1996) A negatively charged anchor residue promotes high affinity binding to the MHC class II molecule I-A^{k}. J Immunol 157: 755–762
58. Gregori S, Trembleau S, Penna G et al. (1999) A binding motif for I-E^{g7}, the MHC class II molecule which protects NOD-Eα transgenic nonobese diabetic mice from autoimmune diabetes. J Immunol 162: 6630–6640
59. Jensen PE (1991) Enhanced binding of peptide antigen to purified class II Major Histocompatibility glycoproteins at acidic pH. J Exp Med 174: 1111–1120

60. Reizis B, Eisenstein M, Mor F, Cohen IR (1998) The peptide binding strategy of the MHC class II I-A molecules. Immunol Today 19: 212–216
61. Marshall KW, Liu AF, Canales J et al. (1994) Role of polymorphic residues in HLA-DR molecules in allele-specific binding of peptide ligands. J Immunol 152: 4946–4957
62. Valitutti S, Muller S, Cella M, Padovan E, Lanzavecchia A (1995) Serial triggering of many T-cell receptors by a few peptide-MHC complexes. Nature 375: 148–151
63. Natarajan SK, Assadi M, Sadegh-Nasseri S (1999) Stable peptide binding to MHC class II molecule is rapid and is determined by a receptive conformation shaped by prior association with low affinity peptides. J Immunol 162: 4030–4036
64. Verreck FA, Vermeulen C, Poel AV et al. (1996) The generation of SDS-stable HLA-DR dimers is independent of efficient peptide binding. Int Immunol 8: 397–404
65. Nelson CA, Petzold SJ, Unanue ER (1994) Peptides determine the life span of MHC class II molecules in the antigen-presenting cell. Nature 371: 250–252
66. Kim DT, Rothbard JB, Bloom DD, Fathman CG (1996) Quantitative analysis of T cell activation. Role of TCR/ligand density and TCR affinity. J Immunol 156: 2737–2742
67. Kanagawa O, Martin SM, Vaupel BA, Carrasco-Marin E, Unanue ER (1998) Autoreactivity of T cells from non-obese diabetic mice: An I-A^{g7}-dependent reaction. Proc Natl Acad Sci USA 95: 1721–1724
68. Parham P (1990) A diversity of diabetes. Nature 345: 662–664
69. Schmidt D, Verdaguer J, Averill N, Santamaria P (1997) A mechanism for the major histocompatibility complex-linked resistance to autoimmunity. J Exp Med 186: 1059–1075
70. Ridgway WM, Ito H, Fassò M, Yu C, Fathman CG (1998) Analysis of the role of variation of major histocompatibility complex class II expression on nonobese diabetic (NOD) peripheral T cell response. J Exp Med 188: 2267–2275
71. Nepom GT (1990) A unified hypothesis for the complex genetics of HLA associations with IDDM. Diabetes 39: 1153–1157
72. Schmidt D, Amrani A, Verdaguer J, Bou S, Santamaria P (1999) Autoantigen-independent deletion of diabetogenic CD4$^+$ thymocytes by protective MHC class II molecules. J Immunol 162: 4627–4636
73. Routsias J, Papadopoulos GK (1995) Polymorphic structural features of modelled HLA-DQ molecules segregate according to susceptibility or resistance to IDDM. Diabetologia 38: 1251–1261
74. Gregori S, Bono E, Gallazzi F, Hammer J, Harrison LC, Adorini L (2000) The motif for peptide binding to the insulin-dependent diabetes mellitus-associated class II MHC molecule I-A^{97} validated by phage display library. Intl Immunol 12: 493–503
75. Santambroglio L, Sato AK, Carven GJ, Belyanskaya SL, Strominger JL, Stern LJ (1999) Extracellular antigen processing and presentation by immature dendritic cells. Proc Natl Acad Sci USA 96: 15056–15061